Integrative and Comparative Biology

Integrative and Comparative Biology, volume 61, number 2, pp. 442–454
doi:10.1093/icb/icab043

Society for Integrative and Comparative Biology

SYMPOSIUM

How to Stick the Landing: Kangaroo Rats Use Their Tails to Reorient during Evasive Jumps Away from Predators

M. Janneke Schwaner,*[,1] Grace A. Freymiller [†,‡] Rulon W. Clark[†] and Craig P. McGowan*[,§]

*Department of Biology, University of Idaho, 875 Perimeter Drive, Moscow, ID 83844, USA; [†]Department of Biology, San Diego State University, 5500 Campanile Drive, San Diego, CA 92182, USA; [‡]Department of Evolution, Ecology, and Organismal Biology, University of California Riverside, 900 University Avenue, Riverside, CA 92521, USA; [§]WWAMI Medical Education Program, 875 Perimeter Drive, Moscow, ID 83844, USA

From the Symposium "An evolutionary tail: Evo-Devo, structure, and function of post-anal appendages" presented at the Annual Meeting of the Society for Integrative and Comparative Biology, Virtual meeting, January 7, 2021.

[1]E-mail: mjschwan@uci.edu

Synopsis Tails are widespread in the animal world and play important roles in locomotor tasks, such as propulsion, maneuvering, stability, and manipulation of objects. Kangaroo rats, bipedal hopping rodents, use their tail for balancing during hopping, but the role of their tail during the vertical evasive escape jumps they perform when attacked by predators is yet to be determined. Because we observed kangaroo rats swinging their tails around their bodies while airborne following escape jumps, we hypothesized that kangaroo rats use their tails to not only stabilize their bodies while airborne, but also to perform aerial re-orientations. We collected video data from free-ranging desert kangaroo rats (*Dipodomys deserti*) performing escape jumps in response to a simulated predator attack and analyzed the rotation of their bodies and tails in the yaw plane (about the vertical-axis). Kangaroo rat escape responses were highly variable. The magnitude of body re-orientation in yaw was independent of jump height, jump distance, and aerial time. Kangaroo rats exhibited a stepwise re-orientation while airborne, in which slower turning periods corresponded with the tail center of mass being aligned close to the vertical rotation axis of the body. To examine the effect of tail motion on body re-orientation during a jump, we compared average rate of change in angular momentum. Rate of change in tail angular momentum was nearly proportional to that of the body, indicating that the tail reorients the body in the yaw plane during aerial escape leaps by kangaroo rats. Although kangaroo rats make dynamic 3D movements during their escape leaps, our data suggest that kangaroo rats use their tails to control orientation in the yaw plane. Additionally, we show that kangaroo rats rarely use their tail length at full potential in yaw, suggesting the importance of tail movement through multiple planes simultaneously.

Introduction

Tails are a common feature of many animal body plans, but their function is highly variable. Animals are known to use tails for a wide variety of locomotor tasks such as propulsion, maneuverability, manipulation, and/or balancing. Terrestrial animals that employ tails for locomotion predominantly use them for maintaining balance. For example, some monkey species use their tail to balance while walking, to grab branches, and to manipulate tools (Erwin 1974; Hickman 1979; Garber and Rehg 1999; Larson and Stern 2006). Cats use their tail for balance during walking and running (Walker et al. 1998), kangaroos use their tail as a "fifth leg" during pentapedal locomotion (O'Connor et al. 2014), and cheetahs use their tail to balance during rapid re-orientation while running (Patel et al. 2016).

Tails may be particularly important for balance in many bipedal animals. Most bipedal hoppers have a similar body plan, with long hindlegs and a relatively long tail (McGowan and Collins 2018). However, the role of the elongated tail can be very different, depending on the species. For example, kangaroos

Advance Access publication May 3, 2021

are the only bipedal hopper, which are reported to use tails for pentapedal locomotion (O'Connor et al. 2014). In addition, these large bipedal hoppers also use their heavy tails to counterbalance the angular momentum of the legs during the areal phase of hopping (Alexander and Vernon 1975). Kangaroo rats, bipedal hopping rodents, are suggested to use their tail predominantly for balancing during hopping (Bartholomew and Caswell 1951) by counteracting the momentum generated by the body in the pitch plane (Moore et al. 2019). However, kangaroo rats also use explosive vertical jumps to evade snakes (Freymiller et al. 2017), and these high-powered jumps can propel them into the air up to 10 times their hip height (Biewener and Blickhan 1988). The rapid take-off is initially important to move the body away from the attacking predator as quickly as possible, but the large vertical impulse of such jumps means that the jumping individual will move ballistically through the air for an extended period. Because the evading kangaroo rat needs to land in a position that facilitates rapid locomotion away from the predator (i.e., they need to land on their hindlegs), orientation while airborne is also of vital importance for successful predator evasion. During the aerial phase, kangaroo rats appear to be able to control their orientation so that they land feet first and can immediately hop away from the predator. Qualitatively, kangaroo rats appear to influence their orientation while airborne by using tail angular momentum to counter the angular momentum of the head and trunk, but this hypothesis has not been examined quantitatively.

One of the key aspects of controlling body orientation while airborne is angular momentum. Angular momentum is constant in the absence of any externally applied torque. Therefore, animals cannot substantially change how their body is rotating once they leave the ground, but they can rotate body parts relative to one another to change orientation. Specifically, a change in angular momentum by one part of the body, relative to the center of mass (COM), requires an equal and opposite change in angular momentum by another part of the body. Any motion of a body mass can be utilized for reorientation or stability, such as tails, arms, or legs. Tails are an obvious body part that could influence these parameters. For example, some lizards use the tail for active control of rotation around the pitch and yaw axes while leaping and gliding (Jusufi et al. 2008; Libby et al. 2012). As kangaroo rats usually retract their legs fully while airborne, they must instead use their long, flexible tails to generate angular momentum in one direction, which in turn must be balanced by the head and trunk segments moving in the opposite direction. Furthermore, by manipulating the effective length of the tail (i.e., moment of inertia [MoI]) throughout the rotation cycle, kangaroo rats can maintain changes in orientation in one direction over the course of multiple tail rotations. This principle is commonly used by athletes such as gymnasts and divers (Yeadon et al. 1990; Yeadon 1990a, 1990b, 1990c; Wooten and Hodgins 1994) and its applications have been explored for use in bio-inspired robotics (Saab et al. 2018).

Although it has been suggested that kangaroo rats use their long tail to influence aerial orientation (Hildebrand 1974), this has neither been experimentally examined nor quantified and very little is known about what role tail length has for orientation. Therefore, in this study we addressed three questions: (1) is orientation change a function of jump height? (2) How do kangaroo rats use their tail to reorient in the yaw plane? and (3) What is the role of tail length in these processes? We hypothesized that orientation is independent of jump magnitude, which would be reflected in no correlation between jump variables and the magnitude of body re-orientation in the yaw plane. We also hypothesized that kangaroo rats use their tail to re-orient the body, which would be reflected in tail and body angular momenta being opposite in direction but equal in magnitude, according to the law of conservation of angular momentum. Lastly, we hypothesized that tail length highly influences rotations, which would be observed in animals maximizing tail length (and therefore MoI) in the yaw plane.

Materials and methods

Study site and animals

Our study site was approximately two miles southwest of the Desert Studies Center in San Bernadino County, CA, USA, as described in Freymiller et al. (2017). Data were collected in June of 2019. All trials were recorded between sunset and sunrise, as desert kangaroo rats (*Dipodomys deserti*) are nocturnal. Desert kangaroo rats were trapped using extra-long Sherman live traps baited with black oil sunflower seeds. Traps were placed close to active burrow systems. Trapped kangaroo rats were marked for short-term identification using unique dark ink markings with Nyanzol fur dye to be able to distinguish between individuals. Animals were marked and measured in the field and immediately released after all data were obtained.

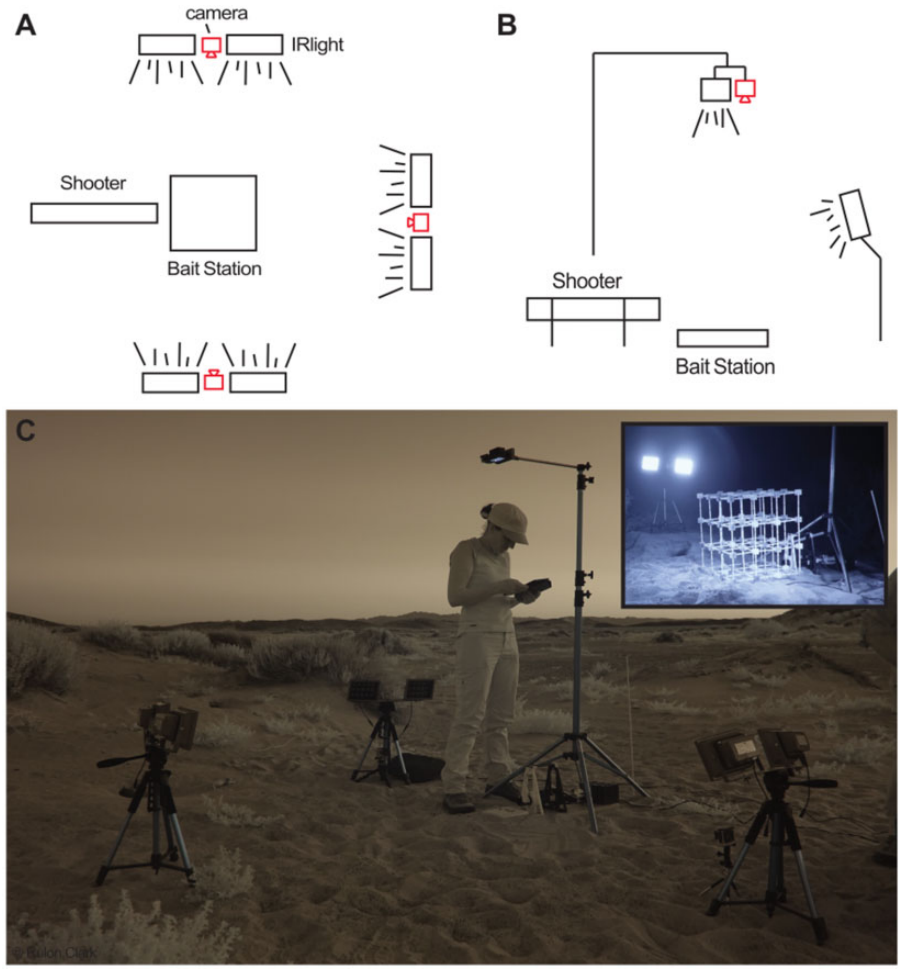

Fig. 1 Experimental set-up. Schematic top view (**A**) and side view (**B**) of equipment set-up (not to scale). Photograph of set-up (**C**) in the field (1.71-m tall researcher for scale) including photograph of calibration frame (right upper corner).

Strike simulator

To evoke an antipredator response, a vertical jump, we used a rattlesnake strike simulator (RSS) adjacent to an active burrow, as based on Freymiller et al. (2017) (Supplementary Video S1). This variation on the original RSS was remotely controlled through a computer tablet by a Bluetooth connection to a small sized computer (Raspberry Pi 4, Raspberry Pi Foundation, Cambridge, UK) that triggered a lever arm to release a string attached to a spring-loaded cork in a tube. Researchers controlled this tablet from 3 to 5 m away. We placed small amounts of sunflower seed in front of the RSS (hereafter "bait station") so that the cork would move rapidly toward any kangaroo rat collecting seed, prompting the animal to jump away from the oncoming stimulus.

Camera set-up

The data collection set-up consisted of four GoPro 4 cameras (GoPro Inc., San Mateo, CA) equipped with infrared (IR) sensitive lens (Fig. 1). Two cameras were placed on either side of the bait station, one in front, and one overhead camera was mounted on a mast that was placed over the RSS. Cameras were recording at approximately 239 frames per second and were continuously collecting data. The 3D space was calibrated with a cube ($480 \times 480 \times 480$ mm) containing 144 markers. After each trial, the calibration frame was placed with a pre-determined unique corner block on the left corner of the raised bait station while recording with all cameras. We recalibrated the 3D space after every potential change in camera position. We provided IR light for each of the cameras (invisible to the kangaroo rats) with two 15 W, 850 NM CCTV Illuminator IR lights (Jing Cheng Digital Surveillance Co., Ltd, Shenzhen, China), that were connected to a 12 V battery. The overhead camera was accompanied with a smaller IR light (HVL-LEIR1, Sony HandyCam Cyber-shot, Sony Corporation, Minota, Japan). Videos were synchronized using a combination of cork movement

and an LED light that turned on as the cork was released from its spring.

Data collection

Kangaroo rats were habituated to feed at the bait station by providing them with small amounts of black oil sunflower seeds. We triggered the RSS when a kangaroo rat moved toward the center of the bait station. After the animal fled, the RSS was reset, and this process was repeated up to 25 times per individual. Multiple individuals were tested by moving the device to different active burrow systems at our site. Although often only one animal would occupy a given site, if additional individuals used a given bait station, we would record trials from multiple individuals at one site.

Analysis

We analyzed physical properties of tails from 10 adult desert kangaroo rat cadavers that were available from a different study. We divided tails into 10 segments from which mass, length (percentage of total length), and the location of the COM were obtained. We measured the rotational inertias of each tail piece using the equation that relates period of a physical pendulum to rotational inertia (Manter 1938, also used in Walter and Carrier 2002; Rankin et al. 2018):

$$I_o = \left(\frac{t}{2\pi}\right)^2 * m * g * d \quad (1)$$

in which I_o is the MoI around the point of oscillation, m the mass of the tail segment, g is the gravitational constant, and d is the distance between the point of oscillation and the segments' COM. The t equals the period of oscillation, obtained from video (Nikon Monarch 5.8 × 48, 400 Hz) of the swinging frozen segment on a string attached to a stiff rod. To determine the MoI around the objects COM we used the parallel axis theorem (Halliday et al. 1993) and the MoI around the point of oscillation (Equation (1)):

$$I_{\mathrm{COM}} = I_o - m * l^2 \quad (2)$$

in which m is the mass of the segment and l the distance of the segments' COM to the point of oscillation. This method was also used to obtain the MoI of the body, which included the legs and head.

Position of the tail COM in the horizontal plane was determined by calculating the X and Y coordinates based on the individual tail segments. For example, x coordinates were calculated as:

$$\mathrm{COM}_X = \frac{(m_1 * X_1) + (m_2 * X_2) + \cdots + (m_{10} * X_{10})}{m_1 + m_2 + \cdots + m_{10}} \quad (3)$$

In which m represents the mass of the given segment and X is the distance from the given segments' COM to the rotation point, the body's COM ($\mathrm{COM_b}$).

From the cadaver data, we obtained tail MoI and determined a relationship between tail length and tail MoI, which was:

$$\mathrm{TailMoI} = 5 * 10^{-7} \times \mathrm{TailLength} - 7 * 10^{-5} \quad (4)$$

In which Tail MoI is the tail's MoI and TailLength is the measured tail length.

Data analysis

Videos of all four camera views were aligned in time and trimmed to the size of single jumping events ($N = 24$ from eight different animals), ranging from 0.38 to 0.92 s per trial (example in Supplementary Video S1). Thirteen markers were digitized on the animal for every camera angle using ProAnalyst (Xcitex Inc., Woburn, MA): nose, left eye, right eye, tail base, tail tip, and eight points on the tail. These tail points were randomly but consecutively selected in a way that the tail curvature was best reflected in the coordinates. As the tail was unmarked, these points varied over the course of a trial, but as they were used to spline through 3D space, it did not have an effect on future analysis. The 3D space was calibrated in ProAnalyst using the measured marker positions of our calibration object, and the resultant spatial coordinate was used to analyze each subsequent video.

Marker data were filtered (third-order Butterworth low-pass filter with a cut-off frequency of 55 Hz) in Matlab (MathWorks, Natick, MA) and the points along the tail, between tail base and tail tip, were interpolated from 8 to 100 points. From the 3D markers of the eyes, nose, and tail base, a "neck" point was calculated. This neck point was placed on the vector between a "mid-eye" point, an imaginary point between the animal's eyes, and the tail base. Based on carcass measurements, the neck point was placed at 15% of the line between this "mid-eye" point and the tail base. A line between the neck point and the tail base was used as a representation of the body, and its orientation. Jump height and distance were calculated based on the maximum displacement of the body COM vertically and horizontally, respectively, from the starting position.

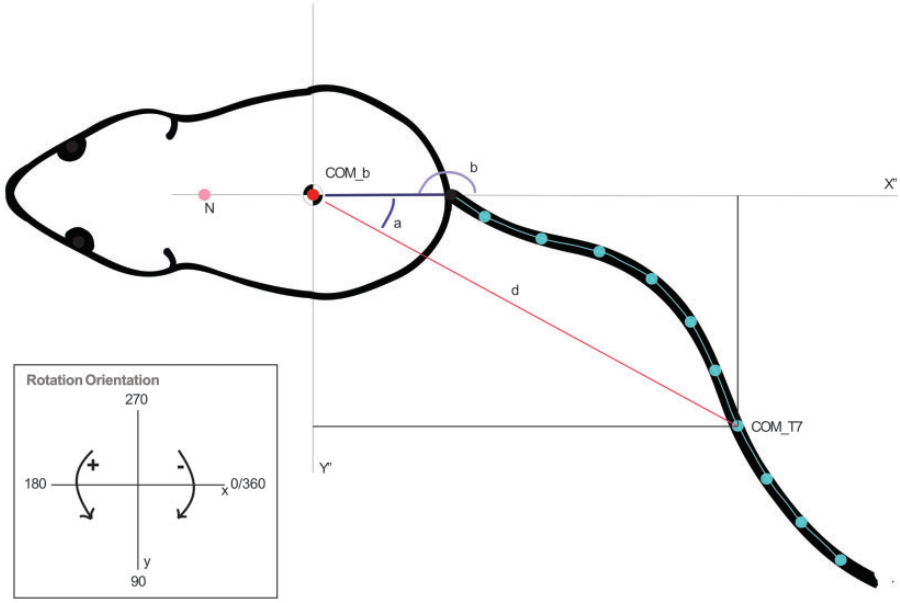

Fig. 2 Schematic of kangaroo rat and tail. The body was represented by a line between the tail base and a neck point (N) on which the COM_b was placed, based on the COM_b measured on animal cadavers. The body angle (b) was calculated between the body and the positive *X*-axis (*X*), represented by parallel axis *X*″ in figure. For each tail segment the distance (d) of that segments' COM to COM_b and the angle with the positive *X*-axis (a) were calculated. In the figure, this is schematically represented for tail segment 7 (T7). *Y*″ represents the parallel Clockwise rotations, increasing angles, were negative, whereas counter-clockwise rotations, with decreasing body angles, were indicated as positive rotations (insert).

Lines were drawn from the COM_b to each of the 10 tail segments' COM (COM_{Ti}) and the identified location of tail COM_T. Angles were calculated between these lines and the positive *X*-axis (Fig. 2). In these calculations, clockwise rotations were identified as negative and counterclockwise rotations as positive (Fig. 2, inset). This angle was used to obtain angular velocity for each tail segment and the whole tail, COM_T. COM_T and COM_{Ti} were modeled as satellites around the COM_b. The tail MoI (T_{MoI}) was calculated as the sum of all tail segment moments of inertia. For each individual tail segment, the MoI (in kg*m^2) was calculated with the following equation:

$$I_{Ti} = m_{Ti} * r_{Ti}^2 \quad (5)$$

in which m is the mass of tail segment i, and r the distance to the COM or segment i to the COM_b.

Angular momenta for COM_b, COM_T, and COM_{Ti} were calculated according:

$$L = \omega * I (6)$$

in which L is the angular momentum, ω is the angular velocity, and I is the MoI of the segment. To obtain the angular momentum of the entire tail (L_{Tsum}), we summed the angular momenta of all individual tail segments. This value of angular momentum was compared to the angular momentum of the body to examine the role of the tail on the body's orientation while airborne. Averages and ranges of angular momentum and angular velocity were calculated and reported as absolute values to combine the analysis of clockwise and counterclockwise turns. Because our main interest was the change in tail and body angular momentum while airborne, initial angular momentum at take-off was used as the starting point of the trial and therefore subtracted from the body and tail angular momentum. Additionally, prior to take-off (but not after), external forces could influence each of these angular momenta. To examine the effects of angular momentum of the tail versus the body during a jump, we compared the average rate of change in angular momentum ($\dot{\bar{L}}$) for each, which is equivalent to the average net torque generated by the motion of each segment. Average rate of change in angular momentum was calculated for each trial by taking the average of the derivative of angular momentum for the tail ($\dot{\bar{L}}_t$) and body ($\dot{\bar{L}}_b$) with respect to time.

Statistical analysis

Statistical analyses on jumping variables and body re-orientation variables were performed with a regression analysis using the statistical toolbox in MATLAB (MathWorks, Woburn, MA), to test correlation between jump height, jump distance, and

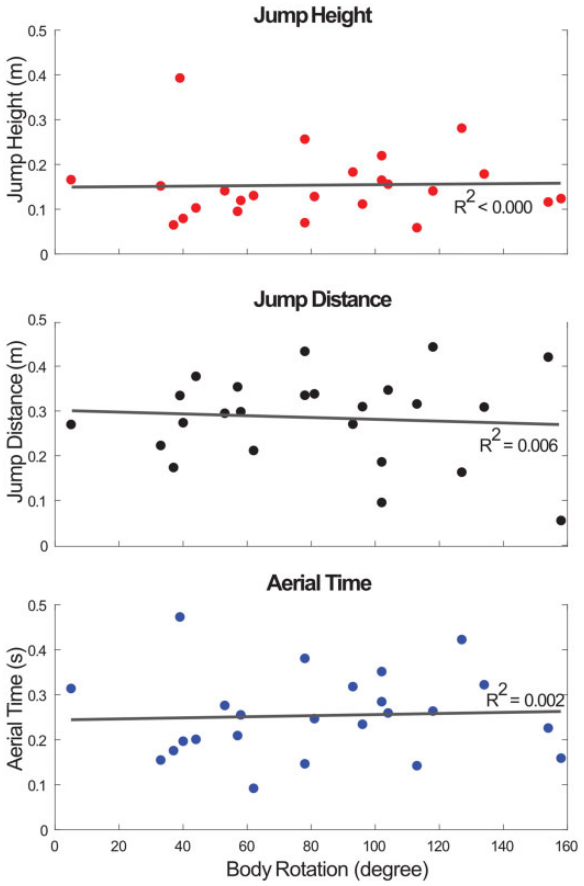

Fig. 3 Jump parameters presented to body rotation during aerial time. For each trial the total body rotation (in degrees) that an animal achieved during the aerial time of the trial was plotted against jump height (**A**), jump distance (**B**), and the time the animal was in the air, or aerial time (**C**). No relationship between body rotation and jump height, jump distance, or aerial time was found ($R^2 < 0.00$; $P = 0.953$, $R^2 = 0.006$; $P = 0.718$, and $R^2 = 0.002$; $P = 0.818$, respectively).

body re-orientation. Averages are presented with ±1 standard deviation (SD). To test correlations between average rate of change in angular momenta of body and tail, a model-II least square fit analysis in MATLAB was used (Pelzer 2016).

Results

Kangaroo rats jumped on average 0.15 m high (±0.07 m) and rotated an average of 81.92 ° (±39.49°) within an average aerial time of 0.25 s (±0.09 s). During these jumps, animals would displace themselves on average 0.28 m (±0.10 m) away from the location where they took off. There was no correlation between total body rotation, measured when the animal was airborne, and jump height ($R^2 < 0.00$, $P = 0.953$; Fig. 3A), jump distance ($R^2 = 0.006$, $P = 0.718$; Fig. 3B), or aerial time ($R^2 = 0.002$, $P = 0.718$; Fig. 3C). From cadaver studies ($n = 10$) of previously obtained animals, we found that average tail length for desert kangaroo rats was 194.66 mm (±8.37 mm) and mass 3.51 g (±0.54 g). Total body mass for these specimens ranged from 87 to 121 g with an average of 105.72 g (±12.86 g). Segment mass decreased with increasing distance from the tail base, reflecting the tapered shape of the tail. Average tail segment masses are reported in Table 1.

Kangaroo rats change orientation angle in the yaw plane (around the *z*-axis) in a stepwise increase or decrease (see Fig. 4A), in which an initial increase in orientation angle was followed by a short period where the angle was stable or even decreased, followed by another increase and angle stabilization. We defined each of these as a re-orientation cycle. Orientation angle stabilization occurred as the tail was close to being aligned to the center of rotation of the body, decreasing the tail's MoI (Fig. 4B and C). To investigate how the tail influences the body's rotation during one full tail rotation, we compared variables from each of these re-orientation cycles.

For each trial, we identified a minimum of one re-orientation cycle and maximum of four re-orientation cycles, with two cycles occurring most frequently (14 times). When re-orientation started before take-off and smoothly increased or decreased until after landing, it was counted as one re-orientation cycle in further analyses. During a re-orientation cycle, animals rotated on average 30.98° away from the RSS (±21.61°) in either direction, ranging from ~2° to ~130°. There was no correlation between jump height and number of re-orientation cycles ($R^2 = 0.046$, $P = 0.312$). Similarly, there was no correlation between jump distance and number of re-orientation cycles ($R^2 = 0.0047$, $P = 0.751$).

There was a positive relationship between change in angle per re-orientation cycle and average tail MoI (Fig. 5A; $R^2 = 0.1454$, $P = 0.0052$). No significant relationship was found between angle change and average tail angular velocity ($R^2 = 0.007$, $P = 0.569$). Over multiple re-orientation cycles, there was no relationship between body angle change and average

Table 1 Average weight for each of 10 tail segments

Tail segment	1	2	3	4	5	6	7	8	9	10
Weight (g)	0.61	0.59	0.55	0.50	0.39	0.30	0.22	0.15	0.11	0.09
SD (g)	(±) 0.100	0.100	0.091	0.088	0.076	0.058	0.039	0.023	0.019	0.023

Tail segments were identified based on percentage of total tail length, so each segment represented 10% of total tail length. Weight decreased when the segment was more posterior on the tail base.

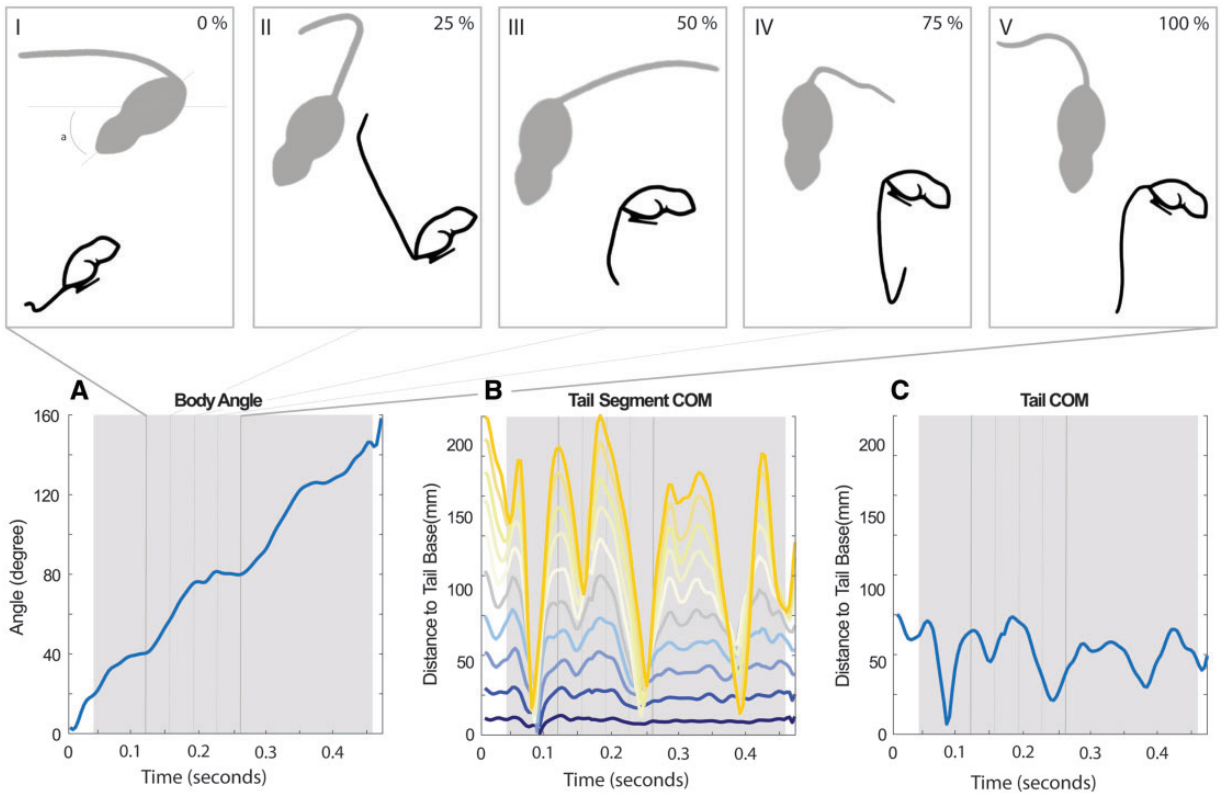

Fig. 4 Body angle (**A**), tail segment COM (**B**), and tail COM (**C**) of a representative trial with corresponding yaw (gray-shaded silhouette) and sagittal plane (outline) view. Gray-shaded area in graphs indicates the period during which the animal is airborne. Body angle (**A**) exhibited a typical "stepwise" pattern during jumping trials. Time of body angle slowing down, occurred simultaneously with the tail segment COMs being close to the tail base (**B**). Distal tail segments were darker blue, whereas more proximal tail segments were dark yellow, all pieces in between were color along shading in between these. The Tail COM (COM_T) also exhibited a relation with relation the body angle change slowing down (**C**), like each individual tail segment. Top row panels indicate respective yaw and sagittal view of animal for a cycle (indicated with vertical solid lines in graphs). Angle (a) is calculated based on horizontal dashed line in panel (I). Each individual panel (I—V) indicates another percentage of the cycle. Location of 25%, 50%, and 75% cycle are indicated with dashed lines in the graph.

tail MoI of the first, second, or third re-orientation cycles ($R^2 = 0.302$, $P = 0.0054$; $R^2 = 0.009$, $P = 0.662$; and $R^2 = 0.041$, $P = 0.745$, respectively; Fig. 5B).

Average angular velocity did not correlate with amount of body rotation per re-orientation cycle (Fig. 5C, $R^2 = 0.007$, $P = 0.569$). There was no relationship between body rotation per re-orientation cycle and angular velocity for either the first, second, or third re-orientation cycle ($R^2 = 0.011$, $P = 0.626$; $R^2 = 0.034$, $P = 0.417$; $R^2 = 0.003$, $P = 0.929$) (Fig. 5D).

Animals left the ground with an average body angular momentum of 0.0011 $kg{\cdot}m^2/s$ ($\pm 0.0011\ kg{\cdot}m^2/s$), ranging from $6.44*10^{-5}\ kg{\cdot}m^2/s$ to $0.004\ kg{\cdot}m^2/s$, and an average tail angular momentum magnitude of $5.99*10^{-4}\ kg{\cdot}m^2/s$ ($\pm 4.52*10^{-4}\ kg{\cdot}m^2/s$), ranging from $7.91*10^{-5}\ kg{\cdot}m^2/s$ to $0.0016\ kg{\cdot}m^2/s$.

Trials with low angular momentum at take-off typically had one or more clearly identified re-orientation cycles (e.g., Fig. 6A). While tails swings were highly variable, a typical cycle began with the tail being swept behind the body, largely in the yaw plane. As the tail reached the body, it was oriented vertically over the body, aligning closely with yaw axis. Peaks in tail angular velocity (Fig. 6B) occurred simultaneously with the tail segments being quickly swept down. This often corresponded with the tail segments being close to vertically aligned to the body's rotation axis in the yaw plane. Therefore, the tail's MoI was low (Fig. 6B, solid line) and had a minimal effect on instantaneous change in angular momentum of the tail (Fig. 6C). In general, tail and body angular momentum mirrored each other (Fig. 6C); however, these variables did not sum to zero for most of the trial (Fig. 6C, dotted line), suggesting other forces may also be contributing.

Trials with high initial body angular momentum at take-off did not have re-orientation cycles. Rather, re-orientation occurred as a continuous change in body angle over a trial (Fig. 7A). In these trials, there

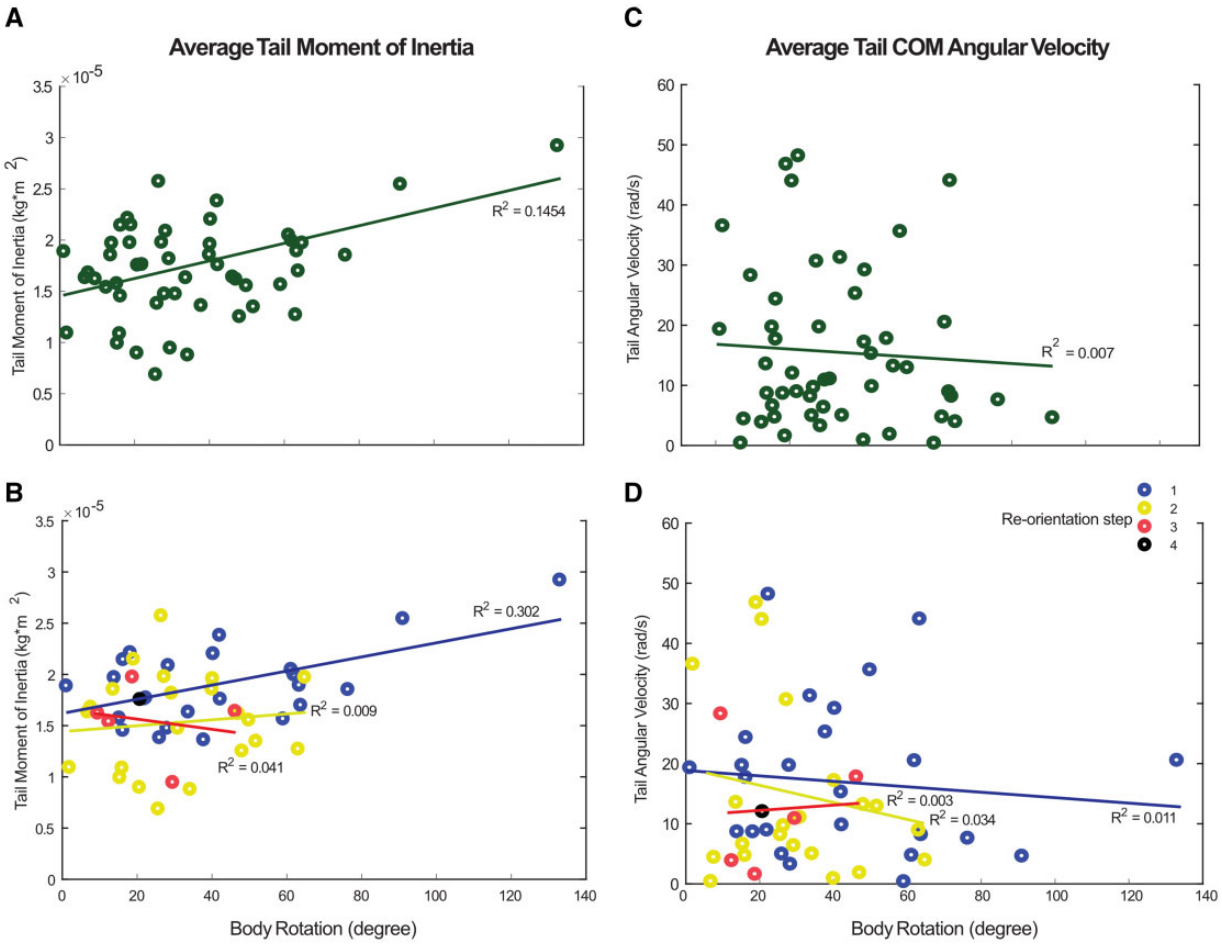

Fig. 5 Average tail MoI (**A and B**) and average angular velocity (**C and D**) for the tail for the body rotation per "re-orientation cycle." (**A**) and (**C**) represent all re-orientation cycles together, whereas (**B**) and (**D**) present those values for the order in which that re-orientation cycle occurred. Neither average tail MoI nor angular velocity had a significant correlation with body orientation over whole trials (**A and C**) (MoI: $R^2 = 0.145$, $P = 0.0053$; Angular velocity: $R^2 = 0.007$, $P = 0.569$). No correlation was found between MoI or angular velocity when discriminating between order of re-orientation cycle (**B and D**) (MoI: $R^2 = 0.302$; $P = 0.0054$, $R^2 = 0.009$, $P = 0.662$, $R^2 = 0.041$, $P = 0.745$. Angular velocity: $R^2 = 0.011$, $P = 0.417$; $R^2 = 0.034$, $P = 0.417$, $R^2 = 0.003$, $P = 0.929$).

was no clear pattern between tail angular velocity and MoI (Fig. 7B), but angular momentum of the tail still largely mirrored the angular momentum of the body (Fig. 7C).

Average time rate of change in angular momentum of the tail was nearly proportional to the rate of change in angular momentum of the body for each trial (Fig. 8). The relationship between body and tail average time rate of change in angular momentum can be expressed as $y = -1.079x - 5.7046{*}10^{-6}$, in which ~60% of variation can be explained by this model ($R = 0.602$). The slope of this relationship, which is close to 1, further supports the finding that tail angular momentum causes direct and opposite changes in body angular momentum.

When comparing over all trials, tail MoI rarely surpassed 80% of maximal tail MoI (Fig. 9). Trials varied in average percent of maximal tail MoI, ranging from 23.26% to 63.24% (±9.24%).

Discussion

Here we show that kangaroo rats use their tail to reorient while airborne, and the magnitude of re-orientation was independent of magnitude of jump variables, in accordance with our hypothesis. The average time rate of change of angular momentum of the tail (i.e., the torque the tail imposes on the body) over a jump was directly proportional to the average time rate of change of angular momentum of the body, suggesting that tail motion controls body re-orientation. Lastly, our data indicate that kangaroo rats rarely use the full potential of their tail's length to maximize tail MoI in yaw. Instead, full

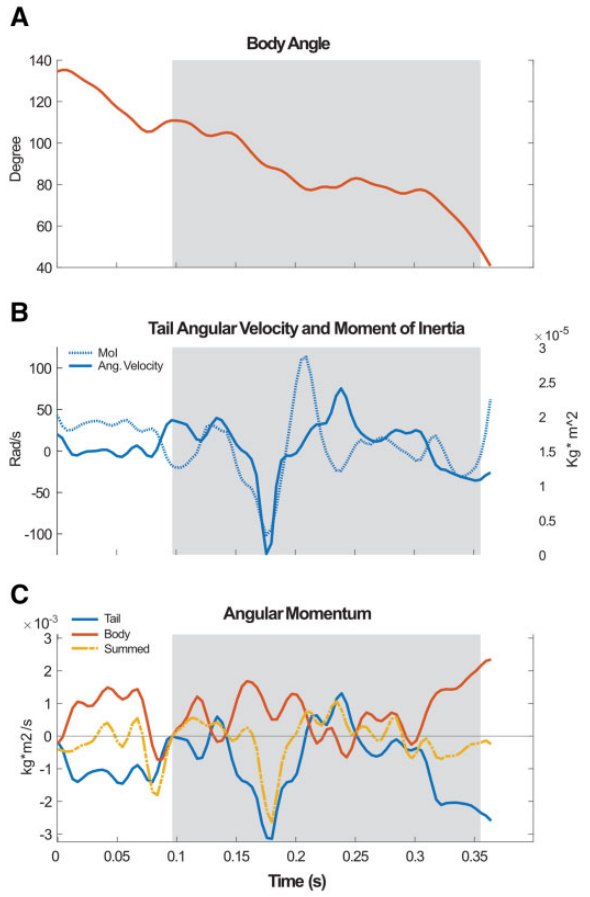

Fig. 6 Body Angle (**A**), tail angular velocity and MoI (**B**) and angular momentum (**C**) for a representative trial with minimal take-off angular momentum. Gray shaded area indicates the period during which the animal is airborne. Body angle (**A**) shows a re-orientation is two re-orientation cycles, with a period around 0.2 s with a less steep decrease in angle, after which it increases the angle change. Tail angular velocity (**B**, solid line) and tail MoI (**B**, dashed line) exhibit a dip in their pattern between 0.15 and 0.2 s. This corresponds with the moment the animal sweeps its tail over the body. Change in angular momentum of the body (**C**, red line) and Tail (**C**, blue line) approximately mirror each other, as indicated by the yellow dashed line which presents the sum of change of body and tail angular momentum (yellow line). Angular momentum for body and tail were zeroed at time of take-off to present change in angular momentum. In this trial, the animal took off with a body angular momentum of $-0.15*10^{-3}$ kg*m^2/s and $1.01*10^{-3}$ kg*m^2/s for the tail.

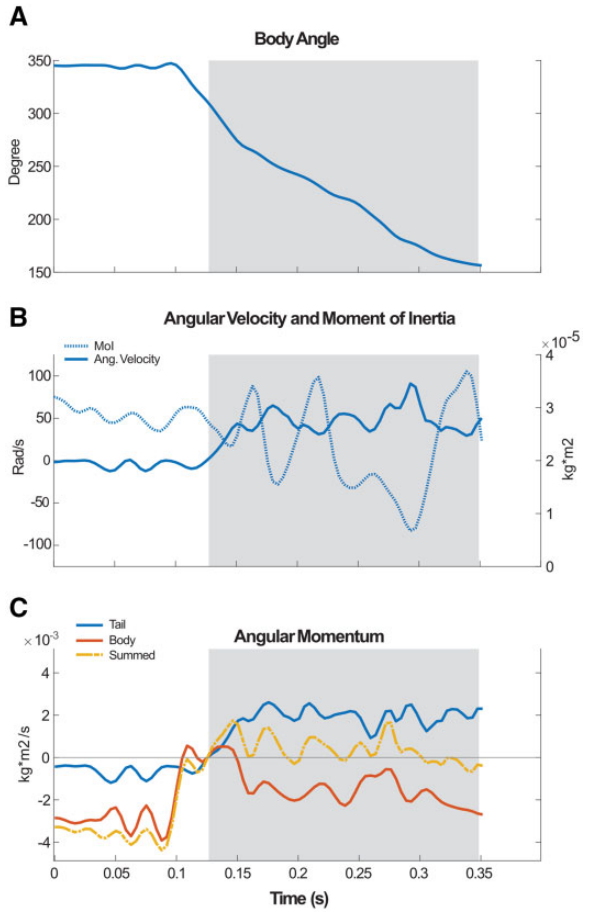

Fig. 7. Body angle (**A**), tail angular velocity, and MoI (**B**) and angular momentum (**C**) for a representative trial with significant take-off angular momentum. Gray-shaded area indicates the period during which the animal is airborne. Body angle (**A**) shows no re-orientation cycles and body rotation is clearly initiated before the animal loses contact with the ground. Tail angular velocity (**B**, solid line) and tail MoI (**B**, dashed line) do not exhibit a clear pattern with respect to the body re-orientation. Change in angular momentum of the body (**C**, red line) and Tail (**C**, blue line) mirror each other, as indicated by the yellow dashed line which presents the sum of change of body and tail angular momentum. Angular momentum for body and tail were zeroed at the time of take-off to present change in angular momentum. At take-off, the body had an angular momentum equal to $2.773*10^{-3}$ kg*m^2/s, whereas the tail had an angular momentum of $0.372*10^{-3}$ kg*m^2/s.

tail length only maximizes occasionally for yaw plane re-orientation, suggesting that the tail influences in all three planes simultaneously.

In our study, kangaroo rats jumped on average 0.15 m vertically and 0.28 m horizontally in response to the RSS. We found no correlation between the magnitude of body re-orientation and any of the jump variables (jump height, jump distance, or aerial time). This suggests that kangaroo rats may actively reorient to a specific target when airborne, while also maintaining roll and pitch control. Alternatively, if kangaroo rats used constant tail sweeps at a fixed velocity while in the air, we would expect re-orientation magnitude to be highly correlated with jumping higher or further. The argument is supported by data from a previous study, in which we found that kangaroo rats mainly re-orient away from the direction where the researchers were sitting while

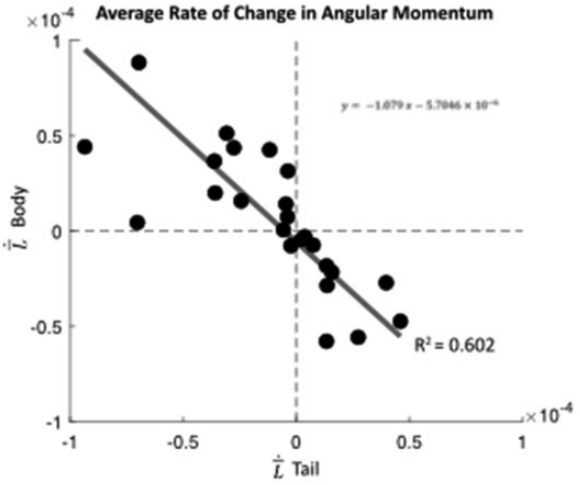

Fig. 8 Average rate of change of angular momentum of tail and body. The average rate of change in angular momentum ((L)) of tail (*X*-axis) and body (*Y*-axis) of all trials and the regression line were plotted. The regression line, with equation in top right graph quadrant, was obtained through a model-II least square fit regression. Data indicate that the re-orientation of the body is proportional to the re-orientation of the tail (regression slope ∼1).

releasing the RSS (Schwaner et al. 2019). Further manipulation of objects and people around the set-up could confirm this finding.

Tail angular momentum occurred in the opposite direction of body angular momentum, but at similar magnitude, which suggests that the kangaroo rat tail is used to reorient the body in the air. For comparison of angular momentum peaks in opposite magnitudes, we compared average time rate of change in angular momentum of the tail and the body, which is equal to the torque that the tail generates on the body during aerial re-orientation. This revealed that the relationship between tail and body average rate of change in angular momentum is close to proportional (slope of 1.07) and that the regression model explains ∼60% of the variation ($R = 0.602$). This supports our hypothesis that kangaroo rats use their tail to reorient while airborne. Similarly, some lizard species are also shown to use their tail to reorient and right themselves in the yaw plane while airborne (Jusufi et al. 2010).

Kangaroo rats re-orientate in cycles rather than effecting a continuous change in angle, which suggests that their aerial body movement is driven by cyclical increases of momentum (such as those produced by a swinging tail). Increases in the tail's MoI in the yaw plane are not consistent over a tail rotation as the tail moves over or under the body; the tail's MoI decreases as it moves close to the body's center of rotation and increases as it moves to the sides, causing cyclical patterns of angular momentum change. This allows the kangaroo rat to re-orient further than can be accomplished with one tail sweep and creates the stepwise re-orientation of the body.

It has been previously suggested that kangaroo rats use their tails for maneuvering while airborne (Bartholomew and Caswell 1951; Hildebrand 1974). Because their tails are disproportionally long compared to body length, they can have a substantial MoI when fully extended, while still having a relatively low mass. However, our data indicate that kangaroo rats rarely maximize their tail's potential of maximal MoI in yaw (Fig. 9). Rather, the full tail length is only occasionally maximized for re-orientation in yaw during the trials we recorded, and it is likely that the tail has a substantial influence on the roll and pitch planes simultaneously. It also appears that angular velocity was not being maximized to control yaw orientation, as peak angular velocity also did not coincide with a peak in the MoI of the tail. Instead, peak angular velocity occurred when the tail was being swept down. More precisely, peak angular velocity coincided with a trough in the MoI as the tail was moved from almost out of the yaw plane (i.e., vertically aligned with the body axis of rotation) to within the yaw plane, a movement which resulted in change from a low functional tail length to a high functional tail length. A possible explanation for this is that kangaroo rats must maintain balance in two more planes (pitch and roll) and maximizing MoI in one plane likely limits the MoI in another plane. In support of this notion, we recorded trials with minimal angle change in the yaw plane but multiple tail rotations, suggesting that kangaroo rats also use their tail for balance in the pitch and roll planes while escaping from predators. During escapes from rattlesnake strikes, kangaroo rats can right themselves mid-air, almost always land on their feet (except for when they have been envenomated and/or are incapacitated by the strike) and will immediately bound away after landing (Higham et al. 2017; Freymiller et al. 2019; Whitford et al. 2019). Thus, kangaroo rats must actively control body orientation in all three planes to execute the landings observed during natural escape responses. Controlling movement in the roll plane will ensure that the kangaroo rat can land on its hind limbs, and control of the pitch plane may additionally serve to ensure that the kangaroo rat lands with an optimal posture and body weight distribution for their next jump, as seen in leaping and reorienting lizards (Jusufi et al. 2008, 2010; Libby et al. 2012). The data we present here is a reference

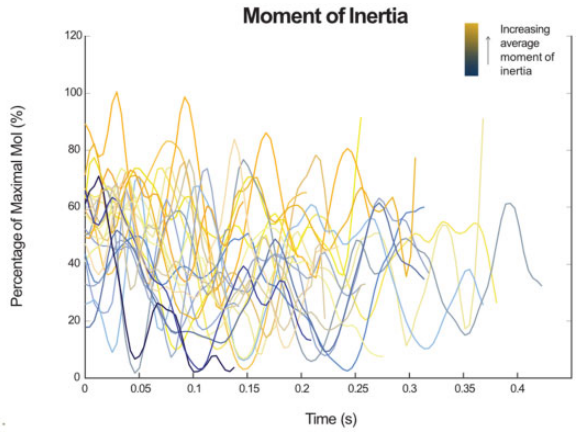

Fig. 9 Tail MoI over all trials. MoI for the tail over trials, colored over a gradient representing average MoI for each trial. Dark blue colors represent low trial tail MoI averages, dark yellow present high tail MoI averages. The maximal tail MoI was calculated from the relationship we found between tail length and MoI, based on cadaver studies (see Materials and methods section for detailed description of this relationship). During most trials, tail MoI does not get >80% of maximum tail MoI.

and framework for future studies investigating the effect of the tail rotations on whole body balance in a multi-planar analysis.

The jumps we report here are substantially lower than what these animals are capable of; kangaroo rats can achieve heights of ~0.8 m off the ground following antipredator jumps away from sidewinder strikes (Freymiller et al. 2019) (see Supplemental Video S2). An earlier study using an RSS to elicit escape responses by desert kangaroo rats also recorded much higher jumps (Freymiller et al. 2017). However, this previous study measured jumps by kangaroo rats that had recently encountered rattlesnakes and recorded data only from the first jump after exposure, when kangaroo rat vigilance was presumably highest. We found, in the absence of a snake, kangaroo rat propensity to jump was highly variable, but when they did jump, their performance was consistent across multiple jumps. The moderate jumps we recorded were also comparable with jumps recorded in laboratory conditions (Schwaner et al. 2018). However, our data also indicate that even moderate jumps require re-orientation while airborne and indicate that high-powered antipredator jumps may be even more reliant on the use of the tail for orientation and landing.

Collecting data from wild, nocturnal animals in the field present some technical challenges and required some assumptions to be made in our analysis. With four cameras capturing the events, we believe that we have similar video quality to that recorded in the lab, but there will always be some level of digitizing error introduced in the analysis. Further, the estimated CoM of the system is unlikely to exactly match the CoM of the body and tail at each instant in time. However, as the tail only presents ~3% of total body weight (Table 1), we are confident that the impact of this on our outcomes was minimal. Lastly, in our calculations of angular momentum of tail and body, we assume no effects of drag. Desert kangaroo rats have a distinct, hairy tuft at the end of their tail, of which the exact purpose still must be determined. It is unlikely that it adds the necessary weight for the tail to be effective as counterbalance for aerial re-orientation, as earlier suggested (Hildebrand 1974); however, it could generate aerodynamic drag forces when swung through the air at velocities observed in this study. The magnitude of these forces is not known, but may contribute to the fact that tail and body angular momentum do not sum to zero. Yet, the near proportional relationship between the rates of change of angular momentum of the body and tail suggest that the drag effects would not substantially alter the main conclusions of this study.

Although kangaroo rats consistently rely on tail movements for balance and re-orientation, limb movement can also balance or influence the body's angular momentum. Kangaroo rats typically tuck their legs close to their body while airborne after jumping, but animals in three trials had extended leg movement throughout. Leg movement may explain some of the variation in the equality between the angular momentum of the body and tail across trials; however, the effects of the legs are likely to be small given that they do not occur predominately in the yaw plane. In addition, kangaroo rats occasionally move their heads relative to their bodies during these escape maneuvers. Although the head has a larger mass than the tail (~22 g, based on cadaver measurements), the MoI is relatively small ($\sim 1.64*10^{-5}\,kg{\cdot}m^2$) and the head never reached high angular velocities. Therefore, we expect that the head would not have a significant effect on body rotation in the yaw plane. However, the head may play a crucial role in the pitch plane, as suggested for lizards during pitching tasks (Libby et al. 2012).

Our data clearly show that the tail is an important element in the re-orientation behaviors that kangaroo rats must accomplish to accelerate in a newly acquired direction after landing. All species of *Dipodomys* are characterized by bipedalism, explosive jumping, and elongated tails. Our data indicate that desert kangaroo rats modulate tail MoI to a greater extent than angular velocity to control body

orientation. Yet, they rarely maximized MoI in the yaw plane. This suggests that these animals' long tails are likely being used to control angular momentum in all three planes simultaneously, and that flexibility may be as important as length. The amount of body re-orientation did not depend on jump distance, jump height, or aerial time, demonstrating that the aerial re-orientation is not a product of these variables and indicating the kangaroo rats may reorient toward targeted directions.

Acknowledgments

The authors would like to thank Emily Zart for assisting with data collection, Dr. Jeff Rankin for helpful comments on analysis, and Brooke Christensen for the kangaroo rat silhouettes in Fig. 4. We also thank the staff at the California Desert Studies Center for facilitating our fieldwork.

Funding

Funding was provided through University of Idaho College of Science (to M.J.S.), American Society of Mammologists (to G.A.F.), and the National Science Foundation # 1553550 (to C.P.M.).

Conflict of interest

The Authors declare that there is no conflict of interest.

Supplementary data

Supplementary data available at *ICB* online.

References

Alexander RM, Vernon A. 1975. The mechanics of hopping by kangaroos (Macropodidae). J Zool 177:265–503.

Bartholomew GA, Caswell HH. 1951. Locomotion in kangaroo rats and its adaptive significance. J Mammal 32:155–69.

Biewener AA, Blickhan R. 1988.Kangaroo rat locomotion: design for elastic energy storage or acceleration? J Exp Biol 212:550–65.

Erwin J. 1974. Laboratory-reared rhesus monkeys can use their tails as tools. Percept Motor Skills 39:129–30.

Freymiller GA, Whitford MD, Higham TE, Clark RW. 2017. Recent interactions with snakes enhance escape performance of desert kangaroo rats (Rodentia: Heteromyidae) during simulated attacks. Biol J Linn Soc 122:651–60.

Freymiller GA, Whitford MD, Higham TE, Clark RW. 2019. Escape dyanmics of free-ranging desert kangaroo rats (Rodentia: heteromyidae) evading rattle snake strikes. Biol J Linn Soc 127:164–72.

Garber PA, Rehg JA. 1999. The ecological role of the prehensile tail in white-faced capuchins (Cebus capucinus). Am J Phys Anthropol 110:325–39.

Halliday D, Resnick R, Walker J. 1993. Fundamentals of physics. New York (NY): John Wiley & Sons, Inc.

Hickman TA. 1979. The mammalian tail: a review of functions. Mammal Rev 9:143–57.

Higham TE, Clark RW, Collins CE, Whitford MD, Freymiller GA. 2017. Rattlesnakes are extremely fast and variable when striking at kangaroo rats in nature: three-dimensional high-speed kinematics at night. Sci Rep 7:40412.

Hildebrand M. 1974. Analysis of vertebrate structure. New York (NY): John Wiley & Sons.

Jusufi A, Goldman DI, Revzen S, Full RJ. 2008. Active tails enhance arboreal acrobatics in geckos. Proc Natl Acad Sci U S A 105:4215–9.

Jusufi A, Kawano DT, Libby T, Full RJ. 2010. Righting and turning in mid-air using appendage inertia: reptile tails, analytical models and bio-inspired robots. Bioinspirat Biomimet 5:045001.

Larson SG, Stern JT. 2006. Maintenance of above-branch balance during primate arboreal quadrupedalism: coordinated use of forearms rotators and tail motion. Am J Phys Anthropol 129:71–81.

Libby T, Moore TY, Chang-Siu E, Li D, Cohen DJ, Jusufi A, Full RJ. 2012. Tail-assisted pitch control in lizards, robots and dinosaurs. Nature 481:181–4.

Manter JT. 1938. The dynamics of quadrupedal walking. J Exp Biol 15:522–40.

McGowan CP, Collins CE. 2018. Why do mammals hop? Understanding the ecology, biomechanics and evolution of bipedal hopping. J Exp Biol 221 (doi: 10.1242/jeb.161661).

Moore JM, McGowan CP, Shine CL, McKinley PK. 2019. Exploring bipedal hopping through computational evolution. Artif Life 25:236–49.

O'Connor SM, Dawson TJ, Kram R, Donelan JM. 2014. The kangaroo's tail propels and powers pentapedal lomotion. Biol Lett 10:20140381.

Patel A, Boje E, Fisher C, Louis L, Lane E. 2016. Quasi-steady state aerodynamics of the cheetah tail. Biol Open 5:1072–6.

Pelzer TE. 2016. TM-file to calculate a "MODEL-2" least squares fit (http://www3.mbari.org/Products/Matlab_shell_scripts/regress/).

Rankin JW, Doney KM, McGowan CP. 2018. Functional capacity of kangaroo rat hindlimbs: adaptations for locomotor performance. J Royal Soc Interface 15:20180303.

Saab W, William SR, Ben-Tzvi P. 2018. Robotic tails: a state-of-the-art review. Robotica 36:1263–77.

Schwaner MJ, Freymiller GA, Whitford MD, Higham TE, Clark RW, McGowan CP. 2019. Tail rotation facilitates active body reorientation during escape responses in kangaroo rats (*D. deserti*). Integr Compar Biol 59:E208.

Schwaner MJ, Lin DC, McGowan CP. 2018. Jumping mechanics of desert kangaroo rats. J Exp Biol 221:jeb186700.

Walker C, Vierck CJ, Ritz LA. 1998. Balance in the cat: role of the tail and effects of sacrocaudal transection. Behav Brain Res 91:41–7.

Walter RM, Carrier DR. 2002. Scaling of rotational inertia in murine rodents and two species of lizards. J Exp Biol 205:2135–41.

Whitford MD, Freymiller GA, Higham TE, Clark RW. 2019. Determinants of predation success: how to survive an attack from a rattlesnake. Funct Ecol 33:1099–109.

Wooten WL, Hodgins JK. 1994. Simulations of human diving. ftp://130.207.127.23/pub/groups/gvu/tr/1994/94-31.pdf (21 August 2020, date last accessed).

Yeadon MR. 1990a. The simulation of aerial movement - I. The determination of orientation angles from film data. J Biomech 23:59–66.

Yeadon MR. 1990b. The simulation of aerial movement – II. A mathematical inertia model of the human body. J Biomech 23:67–74.

Yeadon MR. 1990c. The simulation of aerial movement – III. The determination of the angular momentum of the human body. J Biomech 23:75–83.

Yeadon MR, Atha J, Hales FD. 1990. The simulation of aerial movement – IV. A computer simulation model. J Biomech 23:85–9.